Int. J. Multiphase Flow Vol. 18, No. 3, pp. 413–421, 1992
Printed in Great Britain.

0301-9322/92 \$5.00 + 0.00
Pergamon Press Ltd

THREE-COMPONENT VELOCITY MEASUREMENTS IN A TURBULENT RECIRCULATING BUBBLE-DRIVEN LIQUID FLOW

R. W. GROSS and J. M. KUHLMAN
Mechanical and Aerospace Engineering Department, West Virginia University, Morgantown, WV 26506, U.S.A.

(Received 19 December 1990; in revised form 25 December 1991)

Abstract—Three-dimensional mean and RMS bubble and liquid velocity measurements have been obtained in a turbulent, recirculating, bubble-driven liquid flow. Measurements have been made using a three-component laser Doppler anemometer. Bubble column turbulent liquid circulation for the present experiments is due to injection of a single vertical jet of air along the column centerline. Measured distributions of mean and RMS bubble and liquid velocities are consistent with the existence of a toroidal recirculating liquid flow, as is observed in flow visualization. Measured mean circumferential (swirl) velocity is essentially zero. RMS velocities in all three directions are of the same order of magnitude as the mean velocity, with radial RMS velocity being slightly larger than the other two components. Relative velocities between the bubbles and liquid are significant only near the air jet and near the free surface.

Key Words: bubbly liquid flows, gas–liquid flow, turbulent liquid circulation, laser Doppler anemometry

INTRODUCTION

Efforts to develop, understanding of the dynamics of bubbly gas–liquid flows have led to the use of the laser Doppler anemometer (LDA) as a means of measuring non-intrusively the velocity distributions of both the bubble and liquid phases, at least at low voidages (Durst *et al.* 1984, 1986; Brankovic *et al.* 1984; Sun & Faeth 1986a,b; Currie & Brankovic 1987; Loth & Faeth 1989). One bubbly liquid flow which has broad industrial application is that occurring in a bubble column, where gas bubbles are introduced via nozzles or distributors located at the bottom of the column. A phenomenon termed 'gulf streaming' (Freedman & Davidson 1969) often develops where the liquid circulation, which is driven by the bubble flow, serves to increase both the voidage and the bubble vertical velocity on the column centerline, thereby reducing the gas phase residence time and increasing the required column size.

The present study has extended the laminar flow studies of Durst *et al.* (1984, 1986) into the turbulent flow regime. Measurements have been made of three-dimensional mean and fluctuating bubble and liquid velocities in a recirculating liquid flow, driven by a vertical air jet on the column centerline. The three-component LDA described by Kuhlman & Gross (1989) has been used to obtain the bubble and liquid velocity data non-intrusively. Use of a non-intrusive flow measurement technique is essential for accurate measurements in a recirculating flow, such as the circulation in a bubble column (Durst *et al.* 1984). The present results have been described in greater detail by Gross (1990).

PREVIOUS WORK

Many previous experimental studies of bubble column circulation have used intrusive probes to measure velocities, and generally only vertical velocity has been measured. For example, Hills (1974) utilized resistance and pressure probes to measure radial distributions of voidage and mean vertical velocity for turbulent flow, over a range of gas flow rates. The liquid circulation was observed to be upwards on the column centerline and downwards at large radius, near the column wall. A similar circulation pattern has been measured for a laminar flow in a bubble column with a very small void fraction by Reitema & Ottengraf (1970).

More recently Durst *et al.* (1984) have used a non-intrusive single-channel LDA to determine the mean liquid velocity distribution for an axisymmetric, laminar flow in a cylindrical column. The liquid flow was driven by a single column of discrete bubbles injected at the centerline. Again, a toroidal recirculating liquid flow pattern was measured. Flow visualization photographs clearly indicated that the presence of a probe in their bubble column could alter this liquid circulation from a single recirculation cell, to multiple cells. This demonstrates the need for non-intrusive velocity measurements in the recirculating bubble-driven flow. More recent work (Durst *et al.* 1986) has shown further details of this flow. The present study is a turbulent flow extension of these two studies.

Studies of the bubbly, two-phase flow in a circular pipe have been conducted, for example, by Serizawa *et al.* (1975a,b), van der Welle (1985) and Currie & Brankovic (1987). Serizawa *et al.* (1975a,b) used a series of intrusive probes to measure both mean and turbulence quantities for both the bubble and liquid flows. There was no flow reversal in their vertical pipe, and the flow was driven by an applied pressure difference across the pipe. Radial distributions of axial bubble and liquid velocities and voidage were measured. Resistance probes were also used by van der Welle for bubbly liquid flow for void fractions between 0.25 and 0.75. Radial distributions of void fraction and bubble axial velocity, as well as bubble size, were measured. More recently Currie & Brankovic (1987) obtained axial and radial liquid and bubble velocity measurements for an air–liquid two-phase flow in a vertical pipe with a sudden expansion, using a non-intrusive two-component LDA system. Nouri *et al.* (1987) have used LDA to measure liquid and solid particle mean and RMS axial velocities, both in fully-developed turbulent vertical pipe flow, and for the flow downstream of a baffle. In addition, LDA has been used by Sun & Faeth (1986a,b) and Loth & Faeth (1989) to study the dynamics of bubbly, vertical turbulent jets mixing with a still liquid. Both the bubble and liquid RMS velocities have been measured using LDA in these studies.

EXPERIMENTAL APPARATUS AND PROCEDURE

A schematic of the hexagonal cross-section flow facility is shown in figure 1. The column is made of Plexiglas, is 18 cm across the flats or 21 cm across the diagonal at the top, and can accommodate water depths up to 18 cm from the bubble injection manifold. A series of interchangeable bubble injection manifolds may be installed in the bottom of the column; for the present experiments a manifold drilled with a single, central hole of 1 mm dia has been used. The air flow rate was $7.87 \times 10^{-5} m^3/s$ (10 SCFH). This air flow rate was arbitrary, except that it was judged to be as high as feasible to still allow LDA measurements to be obtained easily with the present apparatus. The shape of this bubble injection manifold is not believed to significantly alter the liquid flow pattern from that resulting from a flush injector with a single, central hole. For the present experiments $Z/(2R) = 0.86$, where Z is the liquid depth from the jet exit. The calculated jet exit air velocity was 90 m/s, so that the superficial gas velocity was only 0.3 cm/s. This resulted in an initial air jet which broke into nominal < 1 cm dia bubbles on the centerline near the top of the column. This air jet drove a relatively strong water circulation, which was observed by flow visualization to be upwards near the central column of air bubbles and downwards near the outer walls of the column. A flow visualization video has indicated the upwards velocity of the air bubbles on the centerline to be between 30–40 cm/s. There was no evidence in the videotape of any meandering of the jet away from the column centerline. This configuration and flow rate have been studied because they greatly simplify the measurement of bubble and liquid velocities, since there is very little interference with the laser beams by bubbles crossing through the beam paths away from where the laser beams cross in the measurement volume to form interference fringes. This is because only the *smaller* bubbles (< 1 mm dia) are re-entrained by the water circulation to recirculate in the column. Note, then, that the present bubble velocity data are actually for these small-diameter bubbles. Also, the hexagonal cross section has been selected because it eliminates the problems associated with optically penetrating a curved interface (Broadway & Karahan 1981; Bicen 1982; Durrett *et al.* 1985), while still remaining nearly cylindrical in cross section.

The present velocity measurements have been obtained using a three-component, five-beam LDA similar to those described by Buchave (1984). This system has previously been used by Kuhlman & Gross (1989) to measure the three-dimensional mean and turbulent velocity fields in an axisymmetric air jet. These jet data were consistent with previous axisymmetric jet data.

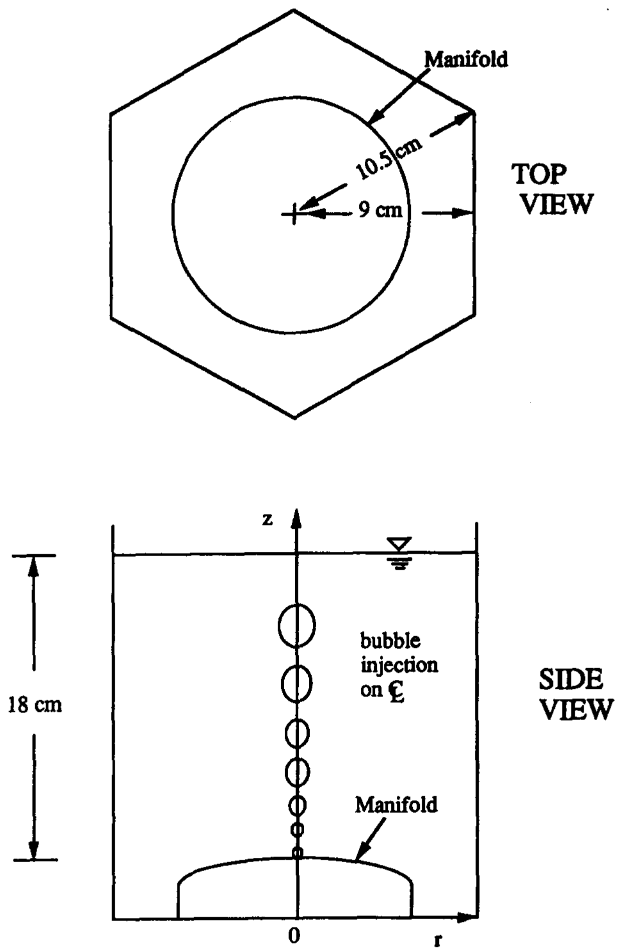

Figure 1. Schematic of the hexagonal cross-section flow facility for LDA measurements.

The LDA system consists of standard DANTEC 55X modular optics and a model 2020 5W Spectra Physics argon ion laser, which are mounted onto a three-dimensional, computer-controlled traversing system, as shown schematically in figure 2. Front lenses with a focal length of 0.6 m are used, so the angle between the two separate optical trains is 60°. This large angle helps to greatly

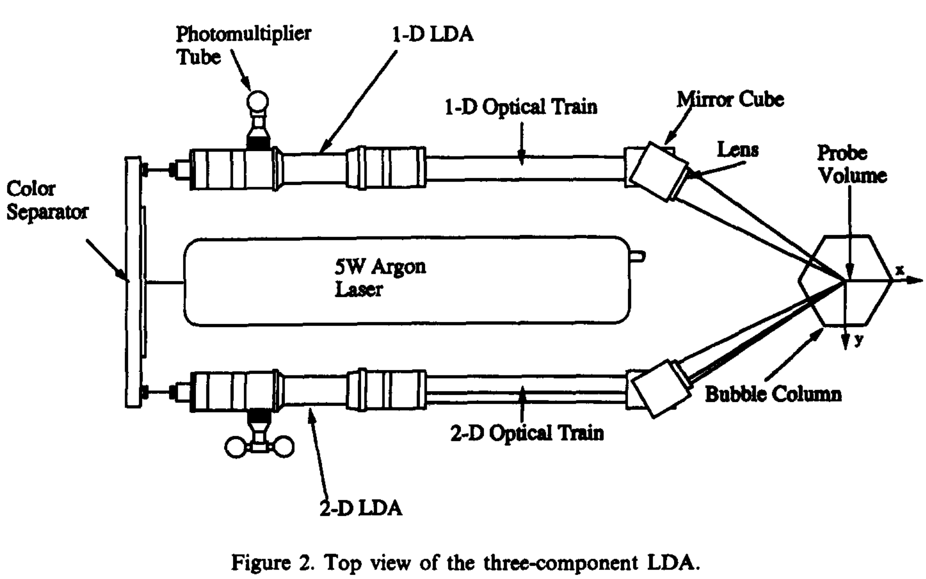

Figure 2. Top view of the three-component LDA.

improve the accuracy of the orthogonal three-dimensional velocity data determined from the non-orthogonal measurements, as discussed by Meyers (1985).

Three separate non-orthogonal LDA channels are formed, by use of color separation. Vertical velocity is measured directly, while the orthogonal horizontal (r–θ) velocity components are computed by vector transformation from the non-orthogonal horizontal velocities to the orthogonal coordinate system. Frequency shifting allows measurements in reversing flows, while beam expanders increase the signal-to-noise ratio. Probe volumes for all three LDA channels are nominally 0.16 mm dia × 3.3 mm long.

All three channels are operated in backscatter. Counter processors are used to measure the Doppler frequency. A special buffer interface may be used to insure that all three velocity measurements occur simultaneously. The present results have been obtained effectively without coincidence of the velocity measurements. Velocity data and the measured time interval between samples are sent to a PDP 11/23 microcomputer for storage. Data is reduced using techniques discussed by Yanta & Smith (1973), Edwards (1987), Meyers (1988) and Gould *et al.* (1989).

Air bubble velocity data have been obtained for a matrix of 20 different vertical depths, by 11 different radial locations. Liquid velocity data have been obtained at the same 20 vertical locations, but at 13 radial locations. These results have been obtained by simultaneously measuring the vertical velocity and one horizontal velocity component perpendicular to one of the column faces, using the two-channel LDA, and then measuring the third velocity component, perpendicular to a neighboring face, at the same location at a later time. Thus, no Reynolds stress results have been obtained. Velocity data obtained from the two non-orthogonal horizontal LDA channels have been post-processed to obtain orthogonal radial and circumferential velocity results. At each location, a time history of 3754 validated LDA velocity measurements has been acquired for each of the three velocity components. Since the counter processors were operated in the 'combined' mode, only one Doppler signal was acquired for each bubble or seed particle that crossed through the probe volume. The sample interval time between each subsequent validated velocity measurement has also been measured. These data have been reduced by sorting the time series for each velocity component into a 100 bin velocity histogram (i.e. number of velocity measurements in each velocity range), and deleting the tails of the resulting histograms for each channel. Between 0.5–8% of the data have been rejected as spurious in this fashion, where for the majority of data files between 1–3% of the data have been omitted by this technique. Average and RMS bubble and liquid velocities have been computed by four different averaging methods: statistical averaging (sum of the velocities divided by number of data values), both with and without rejection of spurious data in the tails of the velocity histograms; and sample interval time weighting, again with and without rejection of spurious data. Very little difference has been observed for these four data reduction methods. The results presented herein have all been calculated using statistical averaging and with the rejection of spurious 'outlier' data. One exception is the two-dimensional air bubble velocity data for the vertical traverse at the third-from-largest r location, where no data rejection was used, since these data files contained fewer samples (from 150 to 2300) due to a lower validated data rate caused by laser beam reflections off the column wall at this radius. Each data record at a point took between 30 and 800 s to acquire, with most files taking 200–300 s. These validated data rates of about 10 samples/s yielded calculated data densities [validated data rate times Taylor microscale; see Edwards (1987)] of between 0.06–0.6. Data densities tended to be higher and fewer spurious points were rejected for the one-dimensional data measurements. For the present results no velocity bias corrections have been applied to the calculated statistical averages (Edwards, 1987; Meyers 1988; Gould *et al.* 1989). This is because velocity bias of the data is not believed to be a significant problem, as a result of the low average validated data rates.

All bubble velocity measurements were obtained using distilled water in the column, with no added seed particles, and without any thresholding of the Doppler signals to reject large signals. Liquid velocity data reported herein have been obtained by adding 4 μm dia silver-coated plastic sphere seed particles (purchased from DANTEC) to the bubble column, and then by rejecting the largest Doppler signals due to the larger air bubbles, through use of a 24 dB threshold setting on each of the counter processors. This level of thresholding was observed to typically reject 90–95% of the Doppler signals obtained without any seed particles added to the flow. Similar use of thresholding to separate Doppler signals from the liquid phase and from the bubbles has been reported by Sun & Faeth (1986a,b) and Nouri *et al.* (1987). The seed particles are expected to adequately track the present flow up to frequencies of 1–2 kHz, based on the work of Hjelmfelt & Mockros (1966). It is expected that other non-intrusive methods, such as phase Doppler techniques (Bauckhage 1985; Drain & Phil 1985), the triple-peak technique (Brankovic *et al.* 1984; Yu & Varty 1988) or fluorescent particles (Goldman & Seasholtz 1988), could lead to better liquid velocity data, but these methods were not available for the present work.

RESULTS

The velocity data herein include the mean and RMS vertical and radial bubble velocity data (unseeded flow; no thresholding), and the companion mean and RMS vertical and radial liquid velocity data (seeded flow with thresholding), at the air flow rate of $7.87 \times 10^{-5}\ m^3/s$ (10 SCFH). All velocity data have been presented vs the non-dimensional effective column radius, r/R, where R is one-half the maximum diameter of the column (21 cm). The circumferential mean velocity data presented by Gross (1990) are essentially zero (< 1 cm/s) throughout the column for both the liquid and bubble velocities. RMS circumferential velocities are quite similar to RMS vertical velocities (Gross 1990).

The mean flow velocity data is consistent with laser light sheet flow visualization (figure 3), where bubbles are observed to rise rapidly near the central air jet, with most bubbles leaving the

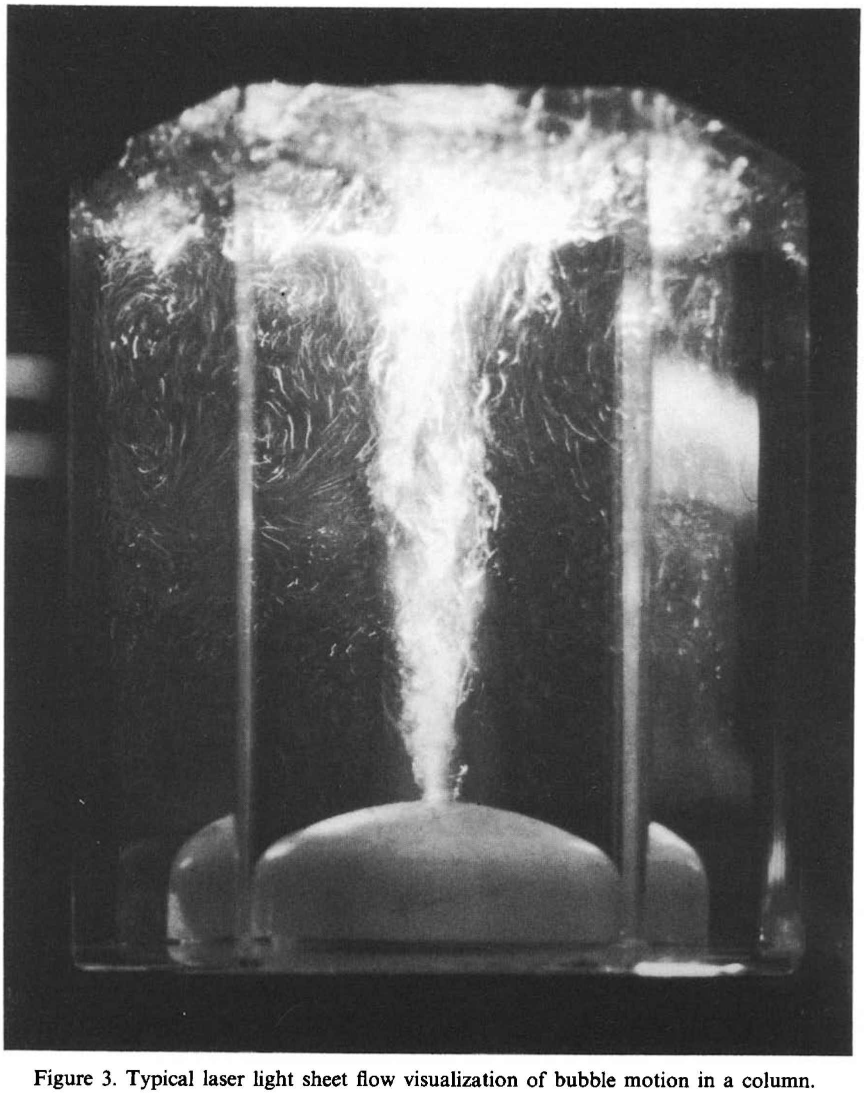

Figure 3. Typical laser light sheet flow visualization of bubble motion in a column.

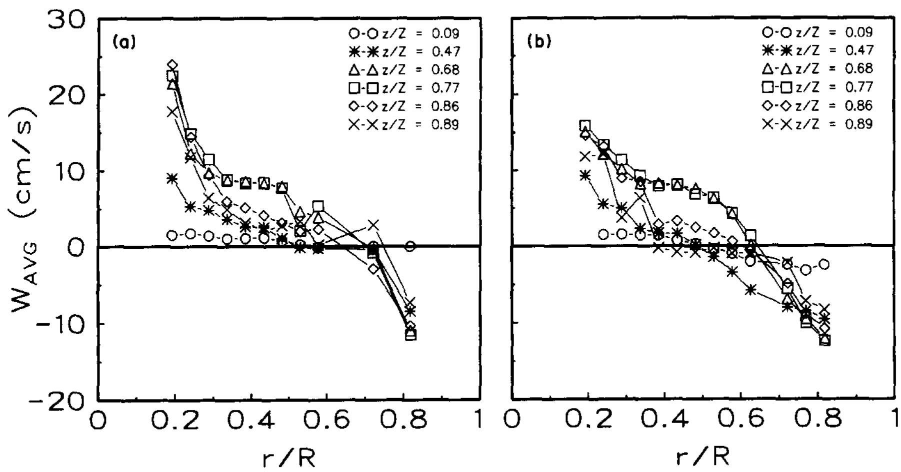

Figure 4. Typical average vertical velocity measurements: (a) bubble data; (b) liquid data.

bubble column at the free surface. Smaller bubbles are observed to move radially outwards near the top of the column, downwards at large r and inwards in the bottom of the column. A relatively strong toroidal recirculating vortex flow is observed in the top half of the column.

No bubble or liquid velocity measurements have been obtained for $r < 0.17R$, because of the presence of the air jet for smaller r. When the probe volume was positioned at the edge of the jet (approx. for $r \cong 0.17R$, or less) the photodetector signals would saturate, or appear extremely 'noisy'. Also, no measurements have been obtained for $r > 0.82R$, since laser light which was reflected off the column walls (water–plastic and plastic–air interfaces) saturated the photodetectors at larger r values. Smaller bubbles which intersected the laser beam paths away from the probe volume reduced signal quality, and eventually destroyed the Doppler signal by destroying the fringe pattern formed in the probe volume (Foster & King 1985).

Typical average bubble and liquid vertical and radial velocity data are presented in figures 4 and 5, respectively, while the corresponding RMS bubble and liquid velocities are shown in figures 6 and 7. Measured velocities are shown vs the non-dimensional radius at several typical values of z/Z, measured relative to the location of the air injection port at the bottom of the column. Additional data at other values of z/Z, shown in Gross (1990), are consistent with the data shown in figures 4–7. The water depth Z, was 18 cm, so $Z/(2R) = 0.86$. Both the mean and RMS velocities are smaller in the bottom half of the column and are largest near the jet (small r) and near the free surface of the column. The circumferential mean velocity is essentially zero everywhere in the

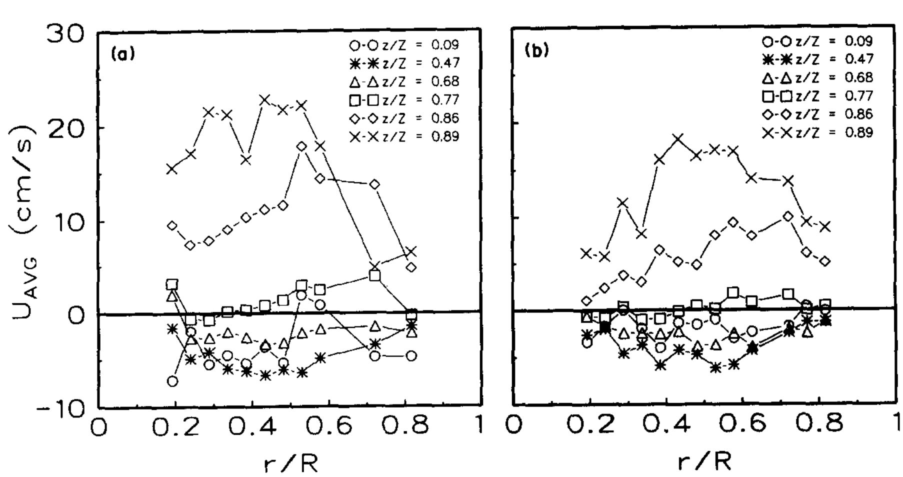

Figure 5. Typical average radial velocity measurements: (a) bubble data; (b) liquid data.

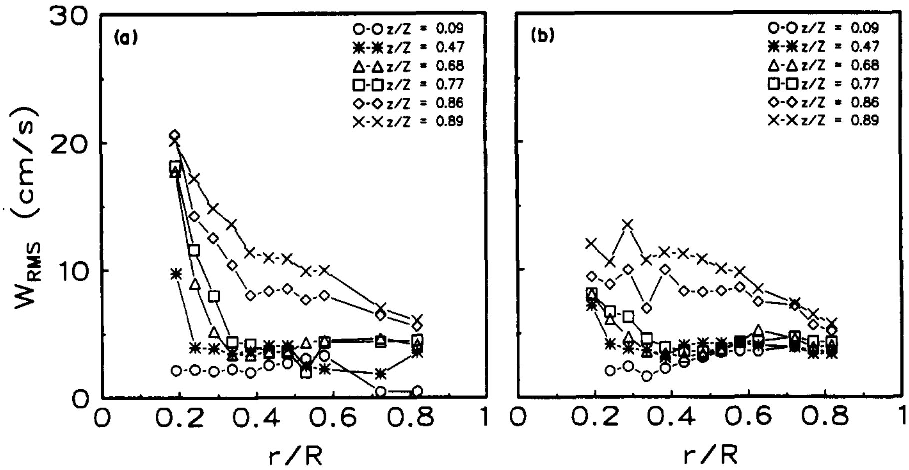

Figure 6. Typical RMS vertical velocity measurements: (a) bubble data; (b) liquid data.

column, as expected (Gross 1990). The vertical mean bubble velocity is largest at a fixed depth for a smaller radius, near the air bubble jet [figure 4(a)]. The vertical bubble velocity is zero at $r \cong 0.7R$ at all depths, upwards for $r < 0.7R$ and downwards for $r > 0.7R$, consistent with a recirculating liquid flow pattern. The mean radial bubble velocity [figure 5(a)] is small and inwards (negative) for the lower three-quarters of the bubble column. However, the mean radial bubble velocity is positive (outwards) in the upper quarter of the column. The outwards bubble velocity near the free surface is the same order of magnitude as the upwards bubble velocity near the air jet. The mean radial velocities appear to go to zero as either the column wall or air jet are approached, as expected.

Liquid velocities follow trends which are similar to observations for the bubble velocities, except that the liquid mean and RMS velocities are generally smaller than the corresponding bubble velocities near the top of the column and near the column centerline. The measured vertical liquid mean velocity is a smaller positive value near the central air jet, and is consistently downwards beyond $r/R \cong 0.5$ to 0.7. These results are expected, since the liquid flow lags behind the bubble flow. Generally, the bubbles move upwards at small r and outwards near the free surface faster than the liquid, as expected. The smallest air bubbles, which are pulled downwards by the liquid circulation at large r and then move radially inwards near the bottom of the column, are seen to move at essentially the same mean velocity as the liquid.

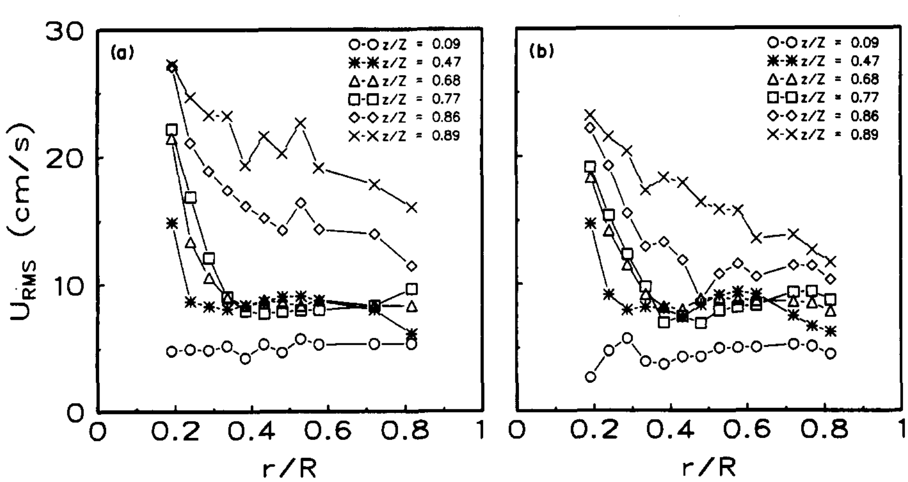

Figure 7. Typical RMS radial velocity measurements: (a) bubble data; (b) liquid data.

Radial RMS velocities (figure 7) are consistently larger than both RMS vertical (figure 6) and circumferential (Gross 1990) velocities, which are generally about the same size. From flow visualization, it has been concluded that this is because much of the fluctuating energy is first fed into the flow due to unsteady motion near the free surface, which is predominantly in the radial direction. In the bottom half of the column, the RMS radial and vertical velocities are essentially the same size as the corresponding mean velocity components. In the top portion of the bubble column, both RMS velocities are closer to the magnitude of the larger of the mean vertical and radial velocities. All RMS velocities decrease as the radius is increased, similar to trends for the mean bubble velocity magnitude. RMS velocities are the same order of magnitude as mean velocities everywhere, indicating very intense local mixing.

CONCLUSION

A series of three-dimensional mean and fluctuating bubble and liquid velocity measurements have been obtained in a turbulent recirculating liquid flow driven by a vertically directed air jet along the column centerline. The data have been obtained non-intrusively using a three-component LDA.

The mean velocity data confirm the existence of a strong, toroidal vortex in the top half of the column, with a much weaker inwards motion in the bottom half of the column. These quantitative data are confirmed by quantitative flow visualization. The circumferential mean velocity is essentially zero. The turbulence field is non-isotropic, as expected, in that radial RMS velocities are generally larger than vertical and circumferential RMS velocities. Significant relative motion between the bubble and liquid phases is observed near the central air jet and near the free surface, where the average bubble size is larger.

The present data extend the range of application of LDA for the study of bubbly liquid flows and contribute to the understanding of the liquid circulation in bubble-driven liquid flows by providing three-dimensional RMS as well as mean velocity data, in a turbulent, recirculating flow. However, it would be beneficial to have a similar data set for a bubble injection manifold which created an initially uniform bubble distribution at the bottom of the column; this would be much more representative of bubble column flows. It is uncertain whether or not LDA can be applied successfully for measurements in such a flow, especially at high voidage, since the presence of bubbles along the optical path away from the LDA probe volume will reduce the signal-to-noise ratio.

Acknowledgements—This work has been supported by DOE Pittsburgh Energy Technology Center under Contract DE-FG22-87PC79935 (Mr Michael Zarochak, Technical Officer). Partial support by the WVU Energy and Water Research Center is also acknowledged.

REFERENCES

BAUCKHAGE, K. 1985 Size, velocity, and flow concentration measurements in sprays by laser-Doppler-anemometry. Presented at the *Int. Conf. on Laser Anemometry—Advances and Applications*, Manchester, U.K., Paper 15.

BICEN, A. F. 1982 Refraction correction for LDA measurements in flows with curved optical boundaries. *TSI Q.* **8,** 10–12.

BRANKOVIC, A., CURRIE, I. G. & MARTIN, W. W. 1984 Laser-Doppler measurements of bubble dynamics. *Phys. Fluids* **27,** 348–355.

BROADWAY, J. D. & KARAHAN, E. 1981 Correction of laser Doppler anemometer readings for refraction at cylindrical interfaces. DISA Information No. 26, pp. 4–6.

BUCHAVE, P. 1984 Three-component LDA measurements. DISA Information No. 29, pp. 3–9.

CURRIE, I. G. & BRANKOVIC, A. 1987 Experimental aspects of turbulent two-phase flow research. Presented at the *2nd Int. Conf. on Laser Anemometry—Advances and Applications*, Strathclyde, U.K., Paper 32.

DRAIN, L. E. & PHIL, D. 1985 Laser anemometry and particle sizing. Presented at the *Int. Conf. on Laser Anemometry—Advances and Applications*, Manchester, U.K., Paper 12.

DURRETT, R. P., GOULD, R. D., STEVENSON, W. H. & THOMPSON, H. D. 1985 A correction lens for laser Doppler velocimeter measurements in a cylindrical tube. *AIAA Jl* **23,** 1387–1391.

DURST, F., TAYLOR, A. M. K. P. & WHITELAW, J. H. 1984 Experimental and numerical investigation of bubble-driven laminar flow in an axisymmetric vessel. *Int. J. Multiphase Flow* **10,** 557–569.

DURST, F., SCHÖNUNG, B., SELANGER, K. & WINTER, M. 1986 Bubble-driven liquid flows. *J. Fluid Mech.* **170,** 53–82.

EDWARDS, R. V. 1987 Report of the Special Panel on Statistical Bias Problems in Laser Anemometry. *ASME Jl Fluids Engng* **109,** 89–93.

FOSTER, S. J. & KING, C. F. 1985 Signal to noise ratio of LDA signals obtained in two-phase flows. Presented at the *Int. Conf. on Laser Anemometry—Advances and Applications*, Manchester, U.K., Paper 28.

FREEDMAN, W. & DAVIDSON, J. F. 1969 Hold-up and liquid circulation in bubble columns. *Trans. Instn Chem. Engrs* **47,** T251–262.

GOLDMAN, L. J. & SEASHOLTZ, R. G. 1988 Three component laser anemometer measurements in an annular cascade of core turbine vanes with contoured end wall. Report NASA TP-2846.

GOULD, R. D., STEVENSON, W. H. & THOMPSON, H. D. 1989 Parametric study of statistical bias in laser Doppler velocimetry. *AIAA Jl* **27,** 1140–1142.

GROSS, R. W. 1990 Laser Doppler anemometry measurements in a laboratory model bubble column. Master's Thesis, Dept of Mechanical and Aerospace Engineering, West Virginia Univ., Morgantown, WV.

HILLS, J. H. 1974 Radial non-uniformity of velocity and voidage in a bubble column. *Trans. Instn Chem. Engrs* **52,** 1–9.

HJELMFELT, A. T. & MOCKROS, L. F. 1966 Motion of discrete particles in a turbulent fluid. *Appl. Sci. Res.* **16,** 149–161.

KUHLMAN, J. M. & GROSS, R. W. 1989 Three component laser Doppler measurements in an axisymmetric jet. Report NASA CR-181908.

LOTH, E. & FAETH, G. M. 1989 Structure of underexpanded round air jets submerged in water. *Int. J. Multiphase Flow* **15,** 589–603.

MEYERS, J. F. 1985 The elusive third component. In *Proc. Int. Symp. on Laser Anemometry*; ASME FED, Vol 33 (Edited by DYBBS, A. & PFUND, P.), pp. 247–254. ASME, New York.

MEYERS, J. F. 1988 Laser velocimeter data acquisition and real time processing using a microcomputer. Presented at the *4th Int. Symp. on Applications of Laser Anemometry to Fluid Mechanics*, Lisbon, Portugal.

NOURI, J. M., WHITELAW, J. H. & YIANNESKIS, M. 1987 Particle motion and turbulence in dense two-phase flows. *Int. J. Multiphase Flow* **13,** 729–739.

RIETEMA, K. & OTTENGRAF, S. P. P. 1970 Laminar liquid circulation and bubble street formation in a gas–liquid system. *Trans. Instn Chem. Engrs* **48,** T54–T62.

SERIZAWA, A., KATAOKA, I. & MICHIYOSHI, I. 1975a Turbulence structure of air–water bubbly flow—I. Measuring techniques. *Int. J. Multiphase Flow* **2,** 221–233.

SERIZAWA, A., KATAOKA, I. & MICHIYOSHI, I. 1975b Turbulence structure of air–water bubbly flow—II. Local properties. *Int J. Multiphase Flow* **2,** 235–246.

SUN, T.-Y. & FAETH, G. M. 1986a Structure of turbulent bubbly jets—I. Methods and centerline properties. *Int. J. Multiphase Flow* **12,** 99–114.

SUN, T.-Y. & FAETH, G. M. 1986b Structure of turbulent bubbly jets—II. Phase property profiles. *Int. J. Multiphase Flow* **12,** 115–126.

VAN DER WELLE, R. 1985 Void fraction, bubble velocity and bubble size in two-phase flow. *Int. J. Multiphase Flow.* **11,** 317–345.

YANTA, W. J. & SMITH, R. A. 1973 Measurement of turbulence—transport properties with a laser Doppler velocimeter. Presented at the *AIAA 11th Aerospace Sciences Mtg*, Washington, DC, Paper AIAA-73-169.

YU, P. Y. W. & VARTY, R. L. 1988 Laser-Doppler measurement of the velocity and diameter of bubbles using the triple-peak technique. *Int. J. Multiphase Flow* **14,** 765–776.